ELSEVIER

Journal of Hazardous Materials 49 (1996) 267–280

JOURNAL OF HAZARDOUS MATERIALS

Distribution study of priority pollutant PAHs from a laboratory aluminum-can chip smelting furnace

Yu-Ling Wei *

Department of Environmental Science, Tunghai University, Taichung, Taiwan

Received 16 May 1995; accepted 10 November 1995

Abstract

In this article, the effect of smelting temperature on the distribution of poly aromatic hydrocarbon (PAH) species in the flue gas streams from a bench-scale laboratory aluminum-can-chip smelting furnace under pyrolytic conditions is examined. The preset smelting temperatures are 600, 700, and 800°C. Both solid-phase and gas-phase PAHs were sampled, extracted, concentrated, and analyzed using GC/FID and GC/MS. Results indicate that increasing furnace temperature increases the species number, average molecular weight, and total concentration of PAHs. Each of the observed PAHs was much more associated with soot particles (i.e., referring as the solid-phase PAHs), compared with what stayed in gaseous form (i.e., the gas-phase PAHs). Further, with the exception of fluoranthene, each PAH's partial pressure in the sampled flue gas stream was much less than its own vapor pressure (i.e., at 25°C). It is proposed that most PAHs are instantaneously wrapped in by the growing soot particles once formed under pyrolytic conditions at high smelting temperatures, thus resulting in the significant difference between each PAH's partial pressure in flue gases and its vapor pressure.

Keywords: Aluminum-can chip smelting; Polyaromatic hydrocarbon; Gas chromatgraphy/mass spectrometry

1. Introduction

The emission of soots during thermal smelting of recyclable aluminum cans has incurred great concern upon public health and the atmospheric environment. PAHs produced during various thermal processes at high temperatures (usually accompanying the soot formation) have also attracted much attention [1–5]. Aluminum smelting processes have been reported to contribute a lot to the total input of PAHs into our

* Corresponding author. Tel: +886-4-3591368, Fax: +886-4-3596858

0304-3894/96/$15.00 Published by Elsevier Science B.V.
SSDI 0304-3894(95)00160-3

living environment. For example, approx. 17% and 54% of the total PAH emissions have been estimated to be from aluminum smelting processes in the USA and Norway, respectively [6].

Often, PAHs containing two to seven aromatic rings may be detected to be associated with soots in the flue gases from combustion, incineration, and other high-temperature processes. In general, these compounds are characterized by low vapor pressures that are in values between 10^{-1} mmHg and 10^{-10} mmHg at 25°C [7], and therefore exhibit higher melting and boiling points than the majority of other organic compounds.

Unfortunately, PAHs in general are mutagenic and/or carcinogenic in nature and their sources can be catalogued into two classes: xenogenetic and anthropogenic ones. The xenogenetic PAH source included biosynthesis activity, nature fire, and so on. Most anthropogenic PAHs are, as previously mentioned, produced from high-temperature industrial activities, and they can be found to exist in the air, water, sludges, and soils of our living environments [8–12]. These toxic pollutants may eventually reach human bodies through the food chains, inhalation of polluted air, etc.

2. Experimental section

2.1. Smelting furnace

The aluminum smelting furnace (Fig. 1) used in this study is made of stainless steel (SS), 60 mm i.d. and 600 mm in height. A piece of round SS plate was welded to one opening end of the SS pipe to support the aluminum-can chip that were to be smelted. To obtain various stable smelting temperatures, a set of temperature controller was

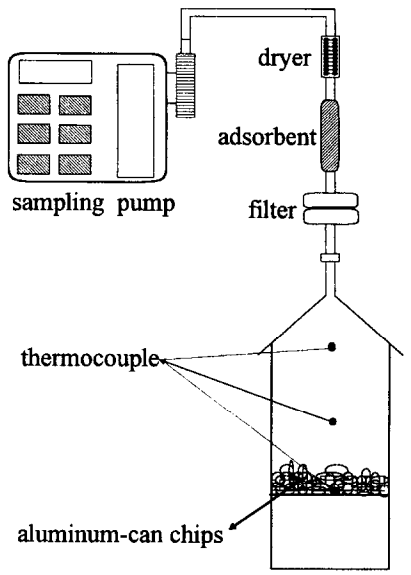

Fig. 1. Smelting furnace and sampling setup.

connected to a thermocouple and a Ni–Cr heating coil that was 2.0 mm in diameter and had an electricity resistance of 0.4297 $\Omega\,m^{-1}$. A thin ceramic insulator was placed between the SS pipe and the Ni–Cr coil to prevent the system from electrical short circuit. Finally, around this Ni–Cr coiled pipe, another piece of ceramic insulator wrapped to keep the electrical heat generated by the Ni–Cr coil from dissipating into atmosphere. In this manner, a preset, stable smelting temperature within the range of 600 and 850°C could be readily achieved.

2.2. Sampling preparation and procedure

From literature, the sampling of PAHs in the flue gases from a fire-tube boiler combustor by adsorbent method was proven to be capable of collecting greater quantity of PAHs than the standard US EPA Method 5 or the High-Volume version of the Method 5 sampling train was [13]. In addition, Jones also reported that the adsorbent method proved itself to be able to give the highest recovery yield of PAHs among all three sampling methods studied [13]. Accordingly, the sampling setup used in this work (Fig. 1) was such arranged that the flue gases (containing soots and PAHs) rising vertically from the aluminum smelting furnace were totally sucked into the collecting funnel, through a filter cartridge containing a 1.0 gm pore size glass fiber filter, and finally through an XAD-2 adsorbent tube and a drying tube in series.

The 1.0 μm pore size glass-fiber filter would intercept most soots in the flue gases, except those with a particle diameter less than 1.0 μm. The XAD-2 tube being connected after the filter cartridge is expected to adsorb all gas-phase PAHs except in the case of a breakthrough condition, under which the quantity of PAHs adsorbed by the rear-section XAD-2 resin is greater than one fifth of that adsorbed by the front-section one. The drying tube following the XAD-2 tube was there for the purpose of protecting the after pump and flow meter.

Prior to sampling, the 1.0 μm pore size glass fiber filter was precleaned in an oven at 350°C for 6 h before being placed in a desiccator at room temperature for 2 days. The XAD-2 adsorbent which is a styrene-divinylbenzene polymer was purchased as a precleaned resin in a sealed glass tube from SKC (USA) and used for sampling without any further pretreatment.

For the sampling procedure, immediately after the smelting furnace reached the preset temperature (i.e., 600, 700, or 800°C), 15 g of aluminum-can chips were batch-admitted to the furnace through the furnace's top opening, the sampling pump was started and the flow rate recorded. After 4 mins of sampling time at a flow rate of 2.1 $L\,min^{-1}$, the extractions of PAHs from the filter and XAD-2 adsorbent were proceeded.

The paint covering the aluminum-can chips consisted of epoxy phenolic, epoxy modified by TiO_2, and polyester types. These compound represented about 10% (by weight) of the chips smelted.

2.3. Sample extraction and pretreatment

As shown in Fig. 2, the collected glass fiber filters and XAD-2 tubes after the sampling procedure required the steps of extracting, rotary-evaporator concentrating,

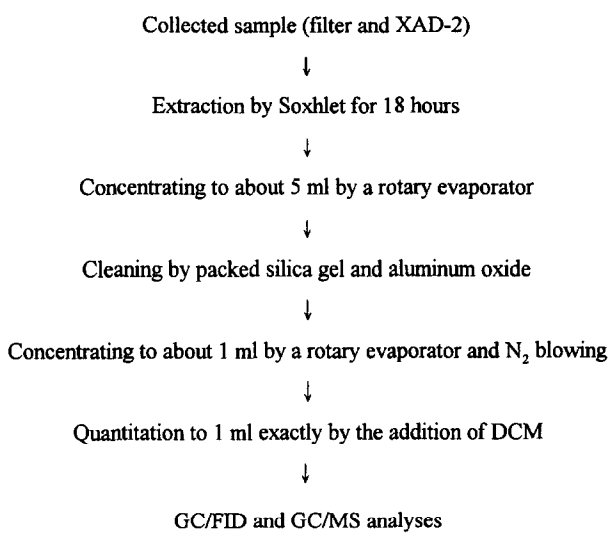

Fig. 2. Sample treatment.

cleaning, re-concentrating by rotary evaporator and N_2 blowing, and diluted to an exact 1.0 ml by dichloromethane (DCM). The so obtained samples (in DCM solvent) were then ready for GC/FID and GC/MS analyses. The identification and quantitation of the 16 priority pollutant PAHs were carried out based upon the retention indeces of the gas chromatograms. A GC/MS was used for auxiliarily qualitative identification of the PAHs.

The standard of the 16 PAHs was purchased as a mixture of solution (Mix 610-M) from Supelco, USA. DCM solvent was chosen for the purpose of extracting PAHs from the collected filters and from the XAD-2 adsorbents due to its characteristics of low boiling point and inertness to a reaction with PAHs [14,15].

The extraction of PAHs from the collected sample was carried out in a Soxhlet extractor. After the extraction step, the feeding of the extract into a pre-cleaning column that was packed with silica gel and activated aluminum oxide pellets, was followed by elutriating an aliquot of 100 ml binary solvent (30% DCM + 70% n-Hexane) to strip the PAHs from the packed silica gel and aluminum oxide. This eluate was then successively concentrated in a rotary evaporator (Heidolph, VV 2000, Germany) and in a cell blown with high-purity N_2 till a volume of slightly less than 1.0 ml was obtained. Finally, the concentrated extract was diluted to an exact 1.00 ml by DCM exactly and ready for GC/FID and GC/MS injections.

The aforementioned packing materials, i.e., the silica gel and aluminum oxide required an activation process in a 150°C oven for 48 h prior to being packed into the pre-cleaning column. 10 g of the activated silica gel and two grams of the aluminum oxide were needed for packing the pre-cleaning column which was 12 mm i.d. and 300 mm in height. To avoid any background contamination, the stationary phase (i.e., packing materials) in the column was subjected to a cleaning step by eluting a 50.0 ml mixture of 30% DCM + 70% n-Hexane before the introduction of the extract.

2.4. GC / FID and GC / MS analyses

Analyses of the extracts were performed with a SHIMADZU Model 14A GC using a 30 m × 0.32 mm i.d. (0.25 μm film thickness) J & W DB-5 capillary column (J & W, USA). The running condition was: injector temperature at 300°C; detector temperature at 310°C; column (oven) temperature starting at 50°C for 2 mins, followed by a temperature ramp at 5°C min^{-1} to 290°C, and staying there for 20 mins; injector port at splitless mode; N_2 carrier gas flow at 1.0 ml min^{-1}; N_2 make-up gas at 40.0 ml min^{-1}; air flow rate at 550 ml min^{-1}; H_2 flow rate at 45.0 ml min^{-1}; and sample injection volume of 1.00 μl. Typical gas chromatograms are depicted in Fig. 3.

GC/MS analyses was performed with a Hewlett–Packard GC Model 5890, using the same capillary column as the GC/FID did and an MS of Model VG Quattro (Fisons Instruments, England) with an ionizing voltage of 70 eV.

2.5. Blank test

Both the XAD-2 adsorbents and the pre-sampled glass fiber filters, after being successively dried in an oven at 350°C and a desiccator for 48 hours, were subjected to the sequential steps of extracting, concentrating, cleaning, re-concentrating, diluting, and analyzing. These sequential steps are exactly the same as those experienced by the used (sampled) filters and adsorbents in order to measure the background content of native PAHs in both the filters and adsorbents.

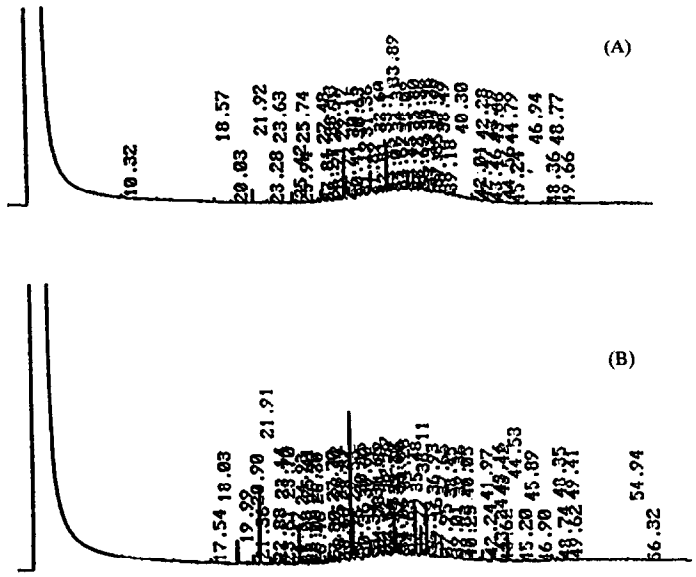

Fig. 3. Typical gas chromatograms: (A) sample from 700°C; (B) sample from 800°C.

2.6. Recovery test

To obtain a general idea about the extent of PAH loss during the steps of extracting, concentrating, cleaning, re-concentrating, and diluting, an aliquot of 1.00 ml PAH standard mixture was spiked into the Soxhlet extractor and underwent through the same sequential steps prior to analyses. The standard mixture contained three components as follows: naphthalene (2-ring), acenaphthene (3-ring), and pyrene (4-ring). Each component is in a concentration of 30.0 $\mu g\,ml^{-1}$ and its recovery percentage is defined as the ratio of the weight recovered to what was originally spiked.

2.7. Chemicals and materials

All chemicals and materials employed in present work were reagent-grade and the usage were not permitted until the background concentrations of the native PAHs had been experimentally determined to be less than the detection limits (DL). The chemicals and materials are described as follows:

Dichloromethane by Mallinckrodt Chrom AR HPLC 99.9% (USA); n-Hexane by Mallinckrodt Chrom AR HPLC 96.9%; Acetone by Mallinckrodt Chrom AR HPLC 99.6%; PAH standard by Supelco, Mix 610-M, Supelco Kit 610-N (USA); Internal standards of 9-methylanthracene and 9,10-diphenylanthracene by TCI (Japan); Silica gel by Riedel-de Hagen, high purity, 70-230 mesh, 63-200 μm (German); Aluminum oxide by Riedel-de Hagen, high purity, 70-290 mesh, 50-200 μm; Glass fiber filter of SKC type A/E, 37 mm d., 1.0 μm pore size (USA); XAD-2 adsorbent tube by SKC, 8 mm o.d. $\times$ 110 mm L. (50/100 mg); Thimble filter by Toyo, Advantec thimble 35 mm $\times$ 120 mm (Japan).

3. Results and discussion

3.1. Standard calibration curve

All correlation coefficients of the standard calibration curves for the 16 PAHs fell between 0.994 and 0.999. The detection limits listed in Table 1 were obtained by the following steps. First, an aliquot of 1.00 μl PAH standard of known concentration that was observed to give a signal to noise ratio (S/N ratio in the GC chromatogram) greater than 3.0 was injected into the GC/FID in seven replicates. Then, the value that was three-fold the standard deviation of the peak area of the seven replicates, was substituted into the area vs. amount linear regression equation (of the standard calibration curve) to give the detection limit for each PAH. It should be noted that all data with GC/FID injections of unknown samples were performed in triplicates in the following paragraphs.

3.2. Recovery test

The validity of spiking PAHs for the routine recovery test has been widely challenged since there was no means to reproduce identical formation mechanisms by which the

Table 1
Detection limit and vapor pressure for standard PAHs

PAH species	Detection limit		Vapor pressure	
	(ng) 25°C	($\mu g Nm^{-3}$) 25°C	($\mu g Nm^{-3}$) 25°C	(mm Hg) [a] 25°C
1 Naphthalene	0.18	15	540000	$7.8 * 10^{-2}$
2 Acenaphthylene	0.11	9.2	55000	$6.7 * 10^{-3}$
3 Acenaphthene	0.17	14	18000	$2.2 * 10^{-3}$
4 Fluorene	0.15	13	5400	$6.0 * 10^{-4}$
5 Phenanthrene	0.21	18	–	–
6 Anthracene	0.13	11	570	$6.0 * 10^{-5}$
7 Fluoranthene	0.02	1.7	–	–
8 Pyrene	0.30	25	49	$4.5 * 10^{-6}$
9 Benzo(a)anthracene	0.66	55	2.6	$2.1 * 10^{-7}$
10 Chrysene	0.27	23	0.08	$6.4 * 10^{-9}$
11 Benzo(b)fluoranthene	0.12	10	–	–
12 Benzo(k)fluoranthene	0.27	23	–	–
13 Benzo(a)pyrene	0.37	31	0.08	$5.6 * 10^{-9}$
14 Indeno(1,2,3-cd)pyrene	1.10	93	–	–
15 Dibenzo(a,h)anthracene	1.70	140	–	–
16 Benzo(g,h,i)perylene	0.40	33	–	–

[a] Ref.[7].

native PAHs are linked to the sample matrices, particularly for the cases of particles formed during combustion (e.g., soots and fly ashes) [16]. The native PAHs are always formed with the sample matrices and are located on less accessible sites throughout the matrices [16]. For soot particles, stronger interaction (adsorption) between the native PAHs and soot matrices, as compared with other matrices, may be expected because of certain similarities of chemical composition. The similarities are that both soots and the native PAHs are carbon-rich organics and the basic structure for them is aromatic rings. Therefore, the recovery tests of PAH-spiked soot particles were not intended in present work. Instead, the recoveries of PAH standards during the steps of extracting, concentrating, cleaning, re-concentrating, and diluting were tested as previously stated in the experimental section.

Only naphthalene (2-ring), acenaphthene (3-ring), and pyrene (4-ring) were selected for the representative recovery tests herein. Table 2 depicts the results of the PAH recovery test. The average recovery percentage (in triplicates) are 80 ± 4, 87 ± 3, and 93 ± 2 for naphthalene, acenaphthene, and pyrene, respectively. As expected, naphtha-

Table 2
Recovery test for the spike of PAH standards

PAH species	Ring number	Average recovery (%), $n = 3$
1 Naphthalene	2	80 ± 4
3 Acenaphthene	3	87 ± 3
8 Pyrene	4	93 ± 2

Table 3
PAH distribution during 600°C smelting run

PAHs species	Solid-phase PAH ($mg\,kg^{-1}$ soot)	XAD-2(f) [a] ($\mu g\,Nm^{-3}$ flue gas)	XAD-2(r) [b] ($\mu g\,Nm^{-3}$ flue gas)
1 Naphthalene		5500 ± 200	< 15
2 Acenaphthylene			
3 Acenaphthene			
4 Fluorene	2730 ± 20		
5 Phenanthrene	9030 ± 340		
6 Anthracene	16500 ± 200		
7 Fluoranthene			
8 Pyrene	3670 ± 30		
Total	31900 ± 400	5500 ± 200	< 15

[a]: front section.
[b]: rear section.

lene recovers least percentage because of the lowest boiling point (218°C) and the highest vapor pressure among three PAHs tested. In a recent article, Burford also reported in high percentage (approx. 70%) loss of naphthalene because of evaporation for 14h after its spiking [16]. The 4-ring pyrene recovers most (93 ± 2 in percentage) since it has the highest boiling point of 404°C and lowest vapor pressure (4.5×10^{-6} mm Hg at 25°C) among the three PAHs tested in this work.

3.3. PAHs formation during aluminum-can smelting

Tables 3–5 present the results of the effect of smelting temperature upon the species distribution of PAHs. There have been some articles discussing the relationship between

Table 4
PAH distribution during 700°C smelting run

PAHs species	Solid-phase PAH ($mg\,kg^{-1}$ soot)	XAD-2(f) [a] ($\mu g\,Nm^{-3}$ flue gas)	XAD-2(r) [b] ($\mu g\,Nm^{-3}$ flue gas)
1 Naphthalene		45800 ± 300	5160 ± 350
2 Acenaphthylene			
3 Acenaphthene	182 ± 61	767 ± 8	
4 Fluorene	4220 ± 310	1070 ± 90	
5 Phenanthrene	17700 ± 400	369 ± 9	
6 Anthracene			
7 Fluoranthene	15400 ± 400	1480 ± 120	612 ± 4
8 Pyrene	11100 ± 400		
9 Benzo(a)anthracene	6880 ± 250		
12 Benzo(k)fluoranthene	2990 ± 40		
Total	58500 ± 800	49500 ± 300	5770 ± 350

[a] Front section.
[b] Rear section.

Table 5
PAH distribution during 800°C smelting run

PAHs species	Solid-phase PAH ($mg\,kg^{-1}$ soot)	XAD-2(f) [a] ($\mu g\,Nm^{-3}$ flue gas)	XAD-2(r) [b] ($\mu g\,Nm^{-3}$ flue gas)
1 Naphthalene		71500 ± 400	16600 ± 100
2 Acenaphthylene			
3 Acenaphthene	1420 ± 70	568 ± 2	
4 Fluorene	11600 ± 400	1010 ± 10	
5 Phenanthrene	51000 ± 800	428 ± 5	
6 Anthracene	25700 ± 100		
7 Fluoranthene	20700 ± 700	1430 ± 30	530 ± 30
8 Pyrene	23500 ± 1000		
9 Benzo(a)anthracene	6600 ± 70		
10 Chrysene	7340 ± 70		
12 Benzo(k)fluoranthene	7180 ± 10		
13 Benzo(a)pyrene	4540 ± 50		
Total	160000 ± 2000	74900 ± 400	17100 ± 100

[a] Front section.
[b] Rear section.

PAH emission rate and combustion (or pyrolysis) temperature. Reported in most papers, the highest emission of PAHs during the combustion of polymers generally occurred at temperatures somewhere within the range of 750°C and 1000°C, regardless of the somewhat different reaction conditions reported by each author [17–20]. Outside this temperature range, either less PAH emissions or non-detectable quantities were reported [17–20]. In present study, as the smelting temperature is increased within the range of 600°C and 800°C, the total emission of the 16 priority pollutant PAHs (either in solid or gas phase) increases. The solid-phase PAHs are defined as what are extracted from the soots, while the gas-phase ones are those from the XAD-2 adsorbents. The emissions of total solid-phase PAHs are $3.19 \times 10^4 \pm 400$, $5.85 \times 10^4 \pm 800$, and $1.60 \times 10^5 \pm 2000$ mg per kg of soot at the smelting temperatures of 600, 700, and 800°C, respectively. The corresponding total gas-phase PAHs are 5.50 ± 0.20, about 55.3 ± 0.5, and about 92.0 ± 0.4 mg per cubic meter of flue gas (at 25°C). If the 16 PAHs are broken down to four individual subgroups based upon the ring number, e.g., 2, 3, 4, and 5 rings, the following discussion on these subgroups becomes somewhat instructive.

For the 2-ring PAH, naphthalene was observed to be 5.50 ± 0.2, 51.0 ± 0.5, and greater than 88.1 ± 0.4 mg Nm^{-3} (a breakthrough of the XAD-2 adsorbent occurred) at smelting temperatures of 600, 700, and 800°C, respectively. Although the XAD-2 tube of the 800°C run was broken through by naphthalene, it may still be concluded that as the smelting temperature increased, naphthalene emission would increase. These concentration of the gas-phase naphthalene can be converted into partial pressure with a unit of mm Hg (at 25°C) via simple calculations. The respective partial pressures are calculated to be $(7.99 \pm 0.29) \times 10^{-4}$ mm Hg, $(7.41 \pm 0.07) \times 10^{-3}$ mm Hg, and slightly greater than $(1.28 \pm 0.01) \times 10^{-2}$ mm Hg for the smelting temperatures of 600, 700, and 800°C.

In contrast, no solid-phase naphthalene was observed for all runs in this study and an explanation for this is proposed as follows. The fate of the native naphthalene, that is simultaneously formed with soot matrices under the pyrolytic condition, can be classified into three types. Naphthalene molecules of the first type are those that act as intermediate species and will further react to produce larger PAHs (greater than 2 rings) or soots. These reactions involve a myriad of free radicals and other intermediate species. Of the second type are naphthalene molecules that diffuse away from the very vicinal environment of the growing soots that are going through the steps of coagulation, aggregation, and agglomeration. The majority of these naphthalene disperses away before any further reaction occurs and whereby become the principal portion of the gas-phase naphthalene. The third type are those that are entrapped in soots and become adsorbed (the solid-phase naphthalene); however, the naphthalene molecules of the third type may either further react at high smelting temperatures to form other species, or diffuse out from the soot particle through the pore tunnels and become gas-phase as a result of their high volatility and smaller molecular radius. Consequently, no observation of solid-phase naphthalene results.

For the case of 3-ring PAHs, the total emissions of the solid-phase PAHs are $(2.83 \pm 0.005) \times 10^4$, $(2.21 \pm 0.05) \times 10^4$, and $(8.97 \pm 0.09) \times 10^4$, mg per kg of soot for the runs of 600, 700, and 800°C, respectively. These results are somewhat surprising that the run at 700°C emits least 3-ring solid-phase PAHs. As far as the gas-phase ones are concerned, none of the 3-ring PAHs was detected during the run at 600°C. In addition, there is only minimal difference in the total yield of the 3-ring gas-phase PAHs between the runs at 700 and 800°C.

For the 4-ring PAHs, an increase in the 4-ring solid-phase PAHs along with the increasing smelting temperature is observed (i.e., $(0.367 \pm 0.003) \times 10^4$, $(3.34 \pm 0.06) \times 10^4$, and $(5.81 \pm 0.12) \times 10^4$ mg kg^{-1} soot for the runs at 600, 700, and 800°C respectively). Concerning the gas-phase ones, none was detected during the 600°C run, and only fluoranthene (of similar quantity) was observed for the runs at 700 and 800°C.

For the 5-ring ones, the 600°C run detected none. The 700°C run emitted only solid-phase benzo(k)fluoranthene in a concentration of $(0.299 \pm 0.004) \times 10^4$ mg kg^{-1} soot. The 800°C run produced $(0.781 \pm 0.001) \times 10^4$ mg of benzo(k)fluoranthene/kg soot, as well as $(0.454 \pm 0.005) \times 10^4$ mg of benzo(a)pyrene/kg soot. None of the 5-ring PAHs was detected in gas phase in this study, presumably becasue of the extremely low vapor pressure that is in the order of 10^{-9} mm Hg at 25°C.

Finally, if the solid-phase PAHs of all rings (3 to 5 rings) are summed up, they are $(3.19 \pm 0.04) \times 10^4$, $(5.85 \pm 0.08) \times 10^4$, and $(16.0 \pm 0.2) \times 10^4$ mg PAHs/kg soot for the smelting runs at 600, 700, and 800°C, respectively. Note that these data can be described by the following regression equation:

$$T = a(\ln M) + b$$

where T and M represent the smelting temperature (K) and the total solid-phase PAHs (3 to 5 rings), respectively; a and b are constants 5.480 and 8.043×10^{-3}, respectively.

Tables 3–5 also illustrates that as the smelting temperature is increased, the total species of PAH increases with a concomitant increase of the average molecular weight (i.e., ring number) of PAHs. The effect of smelting temperature upon the average

molecular weight and the species number of PAHs is perhaps indicative of the PAH formation route based upon the recombination of the free radical fragments formed during the pyrolytic degradation of parent polymer. It is not our purpose to discuss the mechanisms in details; however, a simple discussion of the temperature effect upon PAH formation is as follows.

At the lower smelting temperature of 600°C, the recombination of aromatic hydrocarbons with acetylene is the predominating reaction to give products soots [21] and PAHs; while at 800°C, the formation rate of PAHs is rapidly promoted because of a pyrolytically more reactive environment, largely attributable to the dramatic increase in the number of fragment or reducing radical species, such as H, CH_3, etc. other than acetylene. Therefore, under such pyrolytic conditions at 800°C, the formation of PAHs would proceed in a faster rate than the 600°C run. It should also be noted that during all runs, no air was intentionally pumped into the smelting furnace except some of it might diffuse in from the atmospheric environment; therefore, the concentration of OH radical, compared with the reducing radical species, in the smelting furnace was not high enough to make the oxidative reaction competitive at 600–800°C.

Table 6 summarizes the concentrations of the gas-phase PAHs during the runs at different smelting temperatures, as well as the vapor pressure of PAHs at 25°C. When the comparison between the vapor pressure and the concentrations of gas-phase PAHs of each run is made, one might be curious about the reason that bring about the discrepancy between them, with most of the gas-phase PAH emitted being less than the vapor pressure at 25°C. An explanation is proposed as follows.

The formation of PAHs in this work originates from polymer pyrolysis rather than from the pyrosynthesis of small fuel molecules such as CH_4, C_2H_6, etc.; accordingly, once being formed, the majority of the PAHs might be imagined to be instantaneously wrapped in by the growing soots and only a small portion of the produced PAHs has the opportunity to "escape" from the wrapping behavior of soots. The "wrapped" PAHs may undergo further reactions to form soots, stay non-reacted and adsorbed by specific sites of soots, or diffuse out from soot core through pore tunnels and made a

Table 6
Comparison between gas-phase PAH emission and PAH vapor pressure

PAH species	Gas-phase PAH emission ($\mu g\,Nm^{-3}$ flue gas)			Vapor pressure [a] ($\mu g\,Nm^{-3}$), 25°C
	600°C	700°C	800°C	
1 Naphthalene	5500 ± 200	50960 ± 460	(> 88100 ± 410) [b]	540000
2 Acenaphthylene				55000
3 Acenaphthene		767 ± 8	568 ± 2	18000
4 Fluorene		1070 ± 90	1010 ± 10	5400
5 Phenanthrene		369 ± 9	428 ± 5	–
6 Anthracene				570
7 Fluoranthene		2092 ± 120	1960 ± 40	–

[a] Calculated from Ref. [7].
[b] A slight breakthrough occurred.

contribution to increase the quantity of the gas-phase PAHs. Therefore, if the rates of both PAH wrapping and further reaction (including adsorption) dominate over the rates of "escape" and "diffusion", it would be quite possible that the emission of each gas-phase PAH species during a smelting run will be far less than its vapor pressure at the smelting temperature, or even less than that at 25°C as shown in Table 6.

Nevertheless, caution should be taken to avoid an over-simplified explanation from being made when one tries to explain the formation of PAHs from polymer pyrolysis. Probably, it should be kept in mind that not all types of polymer pyrolysis will necessarily cause effective wrapping of PAHs in soot, neither the "escape" and "diffusion" of PAHs out from soot are absolutely slower processes, compared with the "wrapping" action. Thus, the PAH distribution between the gas phase and the solid phase should be further examined on a case-by-case basis because polymer structure, pyrolytic reaction environment, and other factors would affect the phase distribution of PAHs to some certain extent. Obviously, more researches are needed to fertilize the previous discussion.

For all runs at different smelting temperatures, no acenaphthylene (a 3-ring PAH) was observed at all; while at 700 and 800°C, gas-phase fluoranthene (a 4-ring PAH) was observed to be in quite high partial pressure compared with other 4-ring PAHs. The comparison between the gas-phase partial pressure of fluoranthene and its vapor pressure (mmHg, at 25°C) is not listed in Table 6 because of the non-availability of the vapor pressure. Since neither solid-phase nor gas-phase acenaphthylene was detected, it might be imagined that acenaphthylene was probably formed during the polymer pyrolysis, but then only subject to the immediate subsequent conversion into fluoranthene as well as into soots. As previously mentioned, a detailed discussion of mechanisms for PAH formation is beyond the scope of this article; however, a simple discussion of the conversion from acenaphthene, reacted with C_2H_2, into fluoranthene can be proposed as follows.

As reported in literature, pyrolysis reaction will readily produce species like H, CH_3, CH_4, C_2H_2, C_2H_4, C_2H_6, C_4H_4 and benzene, with the concomitant formation of PAHs [22]. Among these pyrolysis products, C_2H_2 and benzene are considered to be the most persistent ones into the carbon forming region [22]. Further, even tested as a combusted fuel, C_2H_2 was also reported to have a much higher sooting tendency than CH_4, C_2H_4, C_2H_6, and C_3H_8[22]; therefore, this study recognizes that PAHs can act both as intermediate species, for further reaction into soots and PAHs of higher molecular weight, and as final products themselves during the pyrolysis reactions. It is reasonable to propose that acenaphthlene tends to react with active, abundant acetylene to produce fluoranthene at 700 and 800°C under the pyrolytic conditions as experienced in this study (note that both fluoranthene and acenaphthylene were not detected at 600°C). The conversion is roughly indicated as follows:

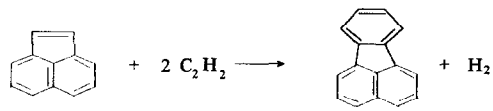

(acenaphthylene) (fluoranthene)

Other than being converted into fluoranthene, acenaphthylene also might react with "hydrogen atom donor" species to form acenaphthene, since the smelting furnace was operated under pyrolytic conditions, where the free radical H and other "hydrogen atom donor" species such as C_nH_m are expected to be at a much higher concentration than OH and O radicals. Even though the H or C_nH_m free radical is less reactive than OH or O, the reduction of the double bond of acenaphthylene (in the five-carbon nonaromatic structure) by the addition of hydrogen atom donor species is still quite possible to occur due to the abundance of hydrogen atom donor and high reaction temperatures, whereby acenaphthlene is converted into acenaphthene as follows:

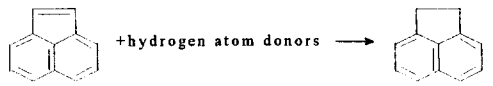

(acenaphthylene) (acenaphthene)

The reaction may proceed via atom transfer reaction that occurs easily at high temperature because of its low activation energy in general.

During the addition reaction of the ethylene-like double bond in the 5-carbon ring structure, the 36 kcal mol^{-1} resonance energy (for a benzenoid ring) tends to stabilize the aromatic naphthalene structure and keep it intact from the hydrogen addition reaction. Or theoretically, the "$4n + 2$" rule for π bonding should be obeyed by a molecule to keep the resonance stabilization effective. To be clear, if all π electrons in the six double bonds of acenaphthylene participated in the resonance stabilization, there would be 12 π electrons (i.e., $6 \times 2 = 12$) as against the $4n + 2$ (i.e., $4 \times 2 + 2 = 10$) rule. Accordingly, the two π electrons of the ethylene-like double bond in the 5-carbon ring structure should not participate in the resonance behavior as the 10 π electrons in the naphthalene structure do, and H addition will most probably occur at the 5-carbon ring structure, whilst the naphthalene structure in acenaphthylene remains intact. In this manner, acenaphthylene is converted into acenaphthene.

4. Conclusion

In present study, the total emission of the 16 priority pollutant PAHs increases as the aluminum-can-chip smelting temperature is increased within the range of 600 and 800°C. The partial pressure of each individual PAH is found to be less than its vapor pressure at 25°C, even though most PAHs are present in very high contents in soots (referred to as solid-phase PAHs).

A quick wrapping in of PAHs by the growing soots is proposed to explain the significant difference between the partial pressure (gas-phase PAHs) and the vapor pressure of PAHs. It is suggested that neither all types of polymer pyrolysis will cause successful wrapping of PAHs inside soots, nor the "escape" and "diffusion" of PAHs out from soot are absolutely slow processes. Thus, the PAH distribution between the gas and solid phases should be examined on a case-by-case basis. More researches are

needed concerning the relationship between the gas/solid PAH distributions and various experimental parameters that include polymer structure, reaction environment, reaction temperature, etc. This will help to clarify the relationship between PAHs and soots during the soot formation processes, especially when whether PAHs are the required intermediates for soot formation still remains in doubt.

Acknowledgements

The laboratory efforts of Miss. Chin-Hua Wu and Mr. Kun-Long Joehuang are gratefully acknowledged. Special thanks are extended to Dr. Chien-Chung Liou for the instrumental work in GC/MS.

References

[1] S.O. Baek, R.A. Field, M.E. Goldstone, P.W. Kirk, J.N. Lester, R. Perry, Water, Air and Soil pollution, 60 (1991) 279.
[2] P.C. Chiang, J.-H. You, S.-C. Chang and Y.-H. Wei, J. Hazard. Mater., 31 (1992) 29.
[3] I.W. Davies, R.M. Harrison, R. Perry, D. Ratnayaka and R.A. Wellings, Environ. Sci. and Technol., 10 (1976) 451.
[4] G. Holmberg and U. Ahlborg, Environ. Health Perspectives, 47 (1983) 1.
[5] K. Yasuda, M. Kaneko, K. Sugiyama, H. Yoshino and Y. Ootsuka, JAPCA, 39 (1989) 1557.
[6] A. Bjoseth and T. Ramdahl, Handbook of Polycyclic Aromatic Hydrocarbons, Vol. 2, Marcel Dekker, Inc., New York, 1985.
[7] B.K. Afghan and A.S.Y. Chau, Analysis of Trace Organics in the Aquatic Environment, CRC Press, Inc., Boca Raton, Florida, 1989, pp. 209–221.
[8] M. Blumer, and W.W. Youngblood, Science, 188 (1975) 53.
[9] P. Wang, V.O. Yen, H.T. Tsai and J.C. Cheng, J. Chin. Chem. Soc., 35 (1988) 13.
[10] E.P. Lankmayr and K. Muller, J. Chromatogr., 170 (1979) 139.
[11] C.A. Menzie, B.B. Potocki and J. Santodonato, Environ. Sci. and Technol., 26 (1992) 1278.
[12] L.S. Deshpande and R. Sarin, Asias J. of Chem. Rev., 2 (1992) 136.
[13] P.W. Jones, R.D. Giammar, P.E. Strup and T.B. Stanford, Environ. Sci. and Technol., 10 (1976) 806.
[14] G.W. Kelly, K.D. Bartle, A.A. Clifford and D. Scammells, J. Chromato. Sci., 31 (1993) 73.
[15] R.N. Westerholm, Environ. Sci. and Technol., 22 (1988) 925.
[16] M.D. Burford, S.B. Hawthorne and D.J. Miller, Anal. Chem., 65 (1993) 1497.
[17] L. Wheatley, Y.A. Levendis, and P. Vouros, Environ. Sci. and Technol., 27 (1993) 2885.
[18] R.A. Hawley-Fedder, M.L. Parsons and F.W. Karasek, J. Chromatogr., 314 (1994) 263.
[19] R.A. Hawley-Fedder, M.L. Parsons and F.W. Karasek, J. Chromatogr., 315 (1995) 201.
[20] R.A. Hawley-Fedder, M.L. Parsons and F.W. Karasek, J. Chromatogr., 315 (1984) 211.
[21] S.K. Ray and R. Long, Combustion and Flame, 8 (1964) 139.
[22] B.S. Haynes and H.G. Wagner, Prog. Energy Combust., 7 (1981) 229.